

Article

# NANO MATERIALS Cite This: ACS Appl. Nano Mater. 2020, 3, 357–363

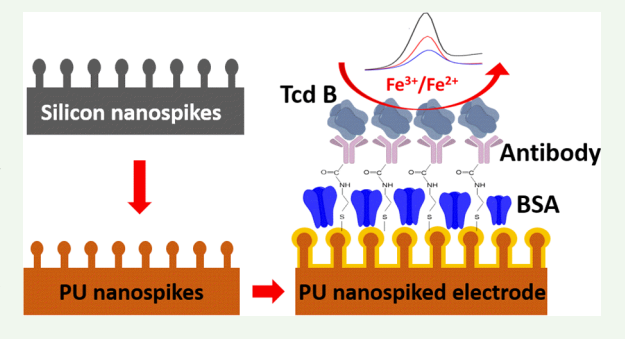
www.acsanm.org

# Disposable Polyurethane Nanospiked Gold Electrode-Based Label-Free Electrochemical Immunosensor for Clostridium difficile

Feiyun Cui, \*\* Zhiru Zhou, \*\* Hanping Feng, \*\* and H. Susan Zhou\*, \*\*

Supporting Information

ABSTRACT: A polyurethane (PU) nanospiked gold electrodebased label-free electrochemical immunosensor for Clostridium difficile (C. difficile) toxin B detection was developed. Different from nanomaterial-modified electrodes, the PU nanospiked gold electrode was fabricated by soft lithography directly. The morphology of the nanospiked electrode was characterized by scanning electron microscope (SEM), and its good electrochemical performance was demonstrated by cyclic voltammetry (CV) as well as differential pulse voltammetry (DPV). Then, the PU nanospiked gold electrode-based immunosensor was developed by fixing antitoxin B single domain antibody on the electrode surface as the receptor. DPV was used as a detection technology for C. difficile



toxin B detection. It revealed that the immunosensor has good specificity, repeatability, and stability. Even in a label-free style, the limit of detection for toxin B was 0.5 pg/mL. In the concentration range of 1–130 pg/mL, the linear regression equation  $\Delta I$ = -1.216[C] -41.62 was found; the correlation coefficient  $R^2$  was 0.9839. Compared with the flat PU electrode-based immunosensor, the detection signal of the PU nanospiked gold electrode-based immunosensor was amplified about 6 times. Benefiting from its low cost and simple processing, the PU nanospiked gold electrode-based immunosensor can be used as a disposable electrochemical sensor for toxin B rapid detection.

KEYWORDS: nanospiked gold electrode, disposable electrochemical sensor, electrochemical immunosensor, C. difficile toxin detection, soft lithography, label-free detection

#### INTRODUCTION

Clostridium difficile infection (CDI) can cause diseases of mild diarrhea and severe pseudomembranous colitis which can result in colectomy and even death. It was responsible for 12.1% of health-care-associated infections (HAI) according to a U.S. prevalence survey. A rapid, simple, accurate, and on-site diagnostic tool is essential to guide therapy and to control transmission. It has been proven that fast positive diagnosis is beneficial for a patient's care by timely isolation and treatment. A negative diagnosis will also result in rapid discontinuation of empirical therapy and isolation.<sup>3,4</sup> Diseases caused by C. difficile infection are mainly due to the release of two exotoxin proteins: toxins A and B (TcdA and TcdB).<sup>5,6</sup> Although detection of toxins or detection of toxigenic organisms remains controversial, many preliminary studies have reported a strong correlation between the severity of the disease and the level of toxins in the stool. It suggested that the detection of toxin concentrations in the stool is clinically valuable in identifying those who need aggressive therapy and predicting treatment

Traditional methods for detecting toxins include cell culture cytotoxicity assay (CTA) and qualitative enzyme immunoassays (EIAs).<sup>7,8</sup> The CTA method requires 24-48 h of incubation, which is too long to obtain outcomes. The EIAs provide relatively fast results. However, many studies showed their lack of sensitivity.8 Because of the above reasons, some novel ultrasensitive C. difficile toxin detection approaches have been reported. Pollock and co-workers developed a digital enzyme-linked immunosorbent assay to determine the C. difficile toxin.9 Sandlund et al. reported an automated single-molecule counting technology for detecting C. difficile toxins A and B. 10 Both of the methods achieved a low limit of detection (LOD). Nevertheless, the approaches need fluorescence labeling, which makes the operation complicated. As we all know, electrochemical biosensors have the advantages of fast response time, high sensitivity, ease of integration, and miniaturization. It has the potential to be a powerful tool for C. difficile toxin rapid and on-site detection. Electrochemical biosensors can be in either label or label-free style. 11 Fang and co-workers developed an electrochemical immunosensor based

Received: October 15, 2019 Accepted: December 26, 2019 Published: December 26, 2019



Department of Chemical Engineering, Worcester Polytechnic Institute, 100 Institute Road, Worcester, Massachusetts 01609, United States

<sup>&</sup>lt;sup>‡</sup>Department of Microbial Pathogenesis, University of Maryland Dental School, 650 W. Baltimore Street, Baltimore, Maryland 21201. United States

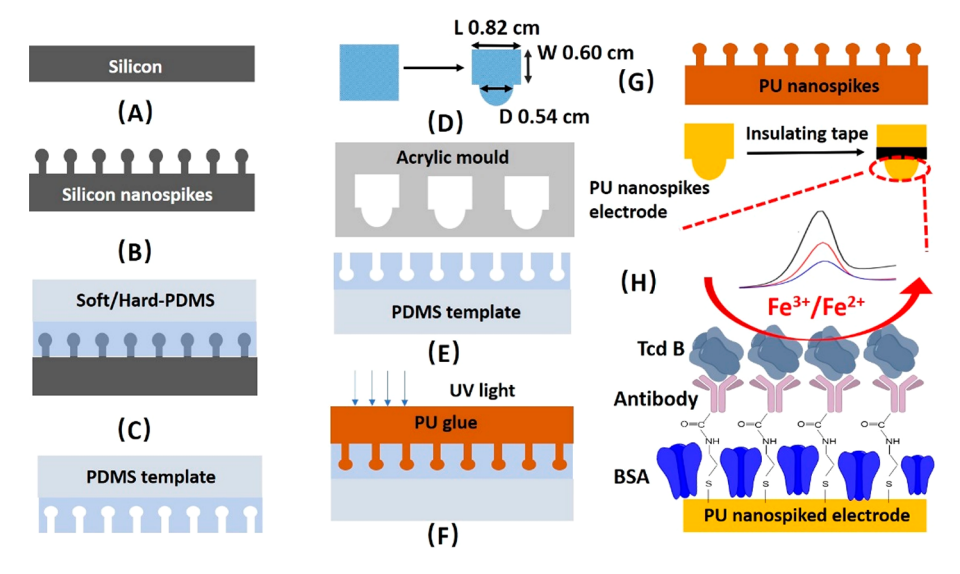


Figure 1. Schematic diagram of the soft lithography preparation steps for PU nanospiked gold electrode and schematic diagram of the electrochemical biosensor. (A) Silicon was irradiated by laser pulses. (B) Form antistiction coating and cast PDMS on nanospiked silicon. (C) Cure PDMS and peel away from the nanospiked silicon. (D) Cut PDMS template into the special shape and fitting them into the acrylic mold. (E) Cast PU glue and cure under UV light for 40 min. (F) Peel away PU nanospikes from PDMS template. (G) Sputter 3 nm Cr and 100 nm Au. (H) Schematic diagram of electrochemical sensor.

on a sandwich type for TcdB detection; they used horseradish peroxidase (HRP) and HRP-Tcd B functionalized graphene oxide (GO) as label agents for signal amplification. Our previous work reported a sandwich-type impedimetric immunosensor for Tcd A and Tcd B measurements; we used single domain  $V_{\rm H}H$  antibody (sdAbs)-coated gold nanoparticles as label material for signal enhancement. Although both of the electrochemical biosensors achieved a low analytical LOD of  $\leq 1~{\rm pg/mL}$ , they are similar to fluorescence-based detection methods and have a relatively complex test process.

Compared with label-based electrochemical biosensors, label-free electrochemical biosensors have the advantages of being simple, having low cost, and having no need to modify the biological samples. They have been widely developed for bioanalysis 14-17 but rarely for *C. difficile* toxin detection. In this study, a label-free electrochemical biosensor for Tcd B detection was developed. What is more, we prepared polyurethane (PU) electrodes with nanospiked surface structure as transducers. Different from most reported nanomaterial-modified electrodes, 18,19 silicon master mold and soft lithography technology were used for preparing this type of polymer nanoelectrode. Owing to their low cost, PU nanospiked gold electrodes can be used for disposable electrochemical sensors.

#### EXPERIMENTAL SECTION

**Materials and Chemicals.** Bovine serum albumin (BSA), hydrofluoric acid (HF, 48%), platinum(0)–1,3-divinyl-1,1,3,3-tetramethyldisiloxane complex solution, 2,4,6,8-tetramethyl-2,4,6,8-tetravinylcyclotetrasiloxane, and trichloro(1H,1H,2H,2H-perfluorooctyl)silane (97%) were purchased from Sigma-Aldrich. Cystamine dihydrochloride (C<sub>4</sub>H<sub>12</sub>N<sub>2</sub>S<sub>2</sub>) was from Fluka. 1-Ethyl-3-(3-(dimethylamino)propyl) carbodiimide (EDC) and N-hydroxysuccinimide (NHS) were from Thermo Scientific. The vinylmethylsiloxane—dimethylsiloxane copolymer, trimethylsiloxy-terminated (VDT-731), and hydrosilane prepolymer (HMS-301) were purchased from Gelest. The recombinant TcdB protein and antibodies (sdAbs) against the TcdB protein were prepared by

methods reported previously. <sup>20,21</sup> The Shiga toxin 2 protein was purchased from Sino Biological Inc. The toxin and antibody solutions were prepared with 0.01 M PBS. The ultrapure water used in our experiment was from a Synergy water purification system (Millipore Sigma).

Hard-poly(dimethylsiloxane) (h-PDMS) and soft-poly-(dimethylsiloxane) (s-PDMS) were prepared as described in ref 22.

Preparation of PU Nanospiked Gold Electrode. Silicon nanospikes were prepared by using femtosecond laser pulses to irradiate the surface of the silicon substrate in distilled water. Then the silicon nanospikes were used as the template for soft lithography. 22,25 The schematic diagram of the preparation steps is presented in Figure 1. First, the silicon nanospikes were immersed in HF (48%) for 2 min and treated by oxygen plasma for 5 min. Then a silane monolayer was formed on the silicon nanospikes by placing several drops of trichloro(1H,1H,2H,2H-perfluorooctyl)silane and silicon nanospikes in a vacuum chamber together. The silane monolayer was used as antisticking layer to decrease the surface energy of silicon nanospikes (Figure 1A). Subsequently, soft/hard PDMS template was prepared by using h-PDMS as a contact layer, and s-PDMS was used as a back layer. Both the thickness of h-PDMS and s-PDMS should be controlled by spin-coating as described in ref 25. The h-PDMS needs to cure at 65 °C for 10 min, and the s-PDMS needs to cure at 65 °C for an additional 2 h in an oven (Figure 1B). After that, the PDMS template was peeled off from the silicon nanospikes (Figure 1C). To make the prepared electrode have a fixed reaction area and match with the electrode hold (PT-3, Gaoss Union), the h-PDMS/s-PDMS templates were cut into a special shape which consists of a rectangle (length 0.82 cm and wide 0.60 cm) and a semicircle (diameter 0.54 cm). The PDMS templates were fit into an acrylic mold and made sure the h-PDMS was on the top side (Figure 1D,E). The PU polymer (NOA 73, Norland Optical Adhesives) was added in the acrylic mold to replicate the nanospiked structures with UV-curing for 40 min (Figure 1F,G). The acrylic mold was used to make the PU nanospikes into the special shape and control the thickness of PU to 2 mm. In this work, about five PU replicas were prepared from the same PDMS template. Subsequently, 3 nm Cr and 100 nm Au films were sputtered on the surface of nanospiked PU (ATC ORION sputtering system, AJA International, Inc.). Insulating tape was used to make sure the semicircle area was fixed as the electrochemistry reaction area.

As a control, flat PU gold electrode was prepared by using the same acrylic mold and sputtering the same Cr/Au films.

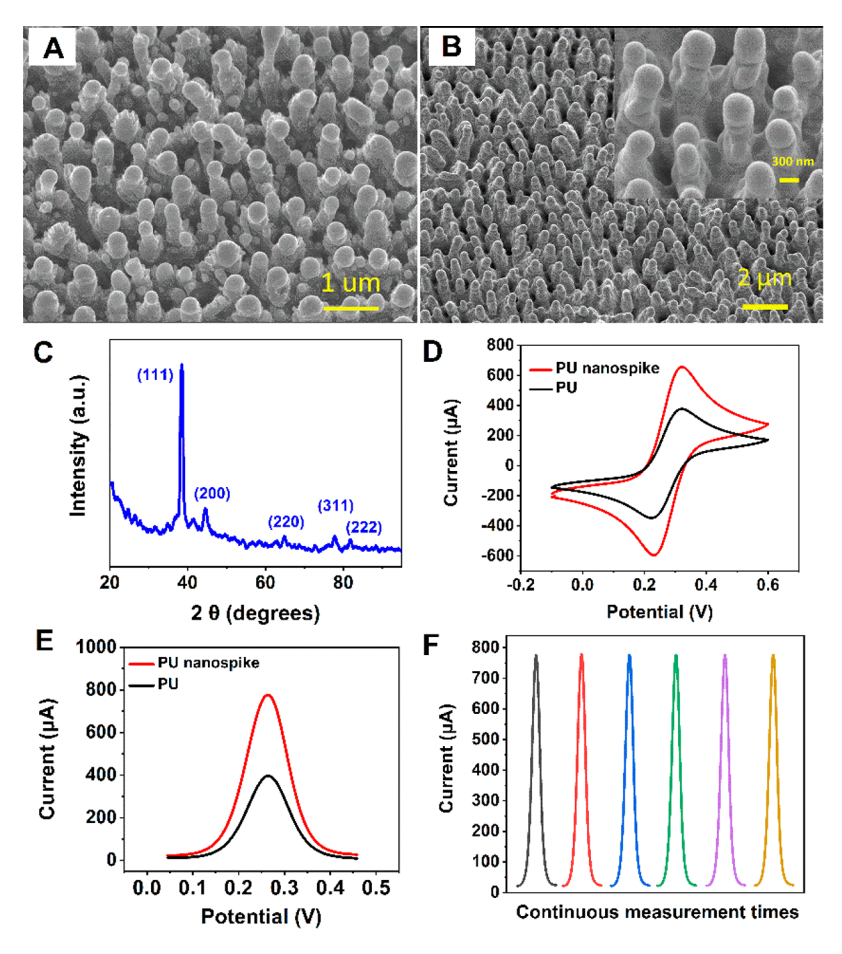


Figure 2. FESEM images of nanospiked silicon substrates (A) and PU nanospiked gold electrode (B); all images were viewed at 35°. (C) XRD spectrum of bare PU nanospiked gold electrode. (D) CV of bare PU nanospiked gold electrode and flat PU gold electrode in 1 M KCl containing 5 mM  $K_3[Fe(CN)_6]/K_4[Fe(CN)_6]$ , with a scan rate of 0.05 V/s. (E) DPV of bare PU nanospiked gold electrode and flat PU gold electrode 1 M KCl containing 5 mM  $K_3[Fe(CN)_6]/K_4[Fe(CN)_6]$ , with a step of 50 mV, a modulation amplitude of 25 mV, a modulation time of 0.05 s, and an interval time of 0.5 s. (F) Six times amplified DPV tests of bare PU nanospiked gold electrode.

Construction of PU Nanospiked Gold Electrode-Based Immunosensor. The cleaned PU nanospiked gold electrode was used as a novel transducer for the immunosensor. Other procedures for construction of the immunosensor refer to our previous work. <sup>13</sup>

**Detection of C. difficile Toxin B.** C. difficile toxin B in 0.5, 10, 40, 70, 100, and 130 pg/mL concentrations were prepared. The immunosensor was incubated with C. difficile toxin B PBS solution from small to large concentrations. We used the 96-hole plate as the reaction container; the volume of Tcd B solution was 300  $\mu$ L. The incubation time was 2 h at room temperature. Then the immunosensor was used as a work electrode to conduct the electrochemical measurements.

**Electrochemical Measurements.** All the electrochemical measurements were conducted by an Autolab PGSTAT12 electrochemical instrument (Metrohm). A three-electrode system was used in this work. The working electrode was a modified PU nanospiked gold electrode, the counter electrode was a platinum wire, and the reference electrode was a saturated Ag/AgCl electrode. Differential pulse voltammetry (DPV), cyclic voltammetry (CV), and electrochemical impedance spectroscopy (EIS) were performed in 1 M KCl containing 5 mM  $K_3[Fe(CN)_6]/K_4[Fe(CN)_6]$ . All the experiments were performed in a Faraday cage.

#### ■ RESULTS AND DISCUSSION

Characterization of PU Nanospiked Gold Electrode. The morphologies of the nanospiked silicon substrates (Figure 2A) and the as-fabricated PU nanospiked gold electrode (Figure 2B) were characterized by a scanning electron

microscope (SEM) (JEOL JSM-7000) with a tilted angle of 35° to the normal surface. As shown in Figure 2A,B, the morphology of the PU nanospiked gold electrode and the morphology of the nanospiked silicon substrate are consistent. Both of them presented spikelike nanostructures with relatively uniform spacing. It showed our method can successfully reproduce the nanostructure of the silicon wafer surface. Because the surface of the PU nanospiked gold electrode was sputtered with 3 nm Cr and 100 nm Au films, the size of the spikes was larger than the size of spikes on the silicon substrate. The elemental composition and phase structures of the PU nanospiked gold electrode were confirmed by using energy dispersive X-ray spectroscopy (EDS, Oxford Instruments NanoAnalysis, USA) and X-ray diffraction (XRD, Bruker AXS D8, USA). The EDS spectrum and mapping of the PU nanospiked gold electrode are shown in Figure S1. As displayed in Figure 2C, all the peaks can be indexed to the Au (111), (200), (220), (311), and (222) crystal faces.

The PU nanospiked gold electrode was characterized by conducting cyclic voltammogram measurement in 0.5 M  $\rm H_2SO_4$  with a scan rate of 50 mV/s and a scan voltage of -0.1 to 1.5 V. Compared with flat PU electrode, the redox peak of the PU nanospiked gold electrode was obviously larger (Figure S2). The CV (Figure 2D) and DPV (Figure 2E) were studied in the -0.1 to 0.6 V range with a scan rate of 0.05 V/s to

characterize the bare PU nanospiked gold electrode. As shown in Figure 2D,E, the current of the PU nanospiked gold electrode was larger than the current of the flat PU. All of them indicate that the PU nanospiked gold electrode had a larger active electrochemical surface area. A larger active area helps to immobilize more antibody molecules and improve the analytical performance of electrochemical sensors, such as sensitivity, linear range, and detection limit.<sup>26</sup> To prove the stability of the PU nanospiked gold electrode, six groups of differential pulse voltammograms of the same electrode were continuously measured. The DPV plot shown in Figure 2F reveals that the prepared PU nanospiked gold electrode exhibited good electrochemical stability. The stability of the electrode was also evaluated by CV with 50 scans. The results show that the stability of the PU nanospiked gold electrode was good. It is enough for the disposable electrochemical sensor (Figure S3).

Electrochemical Characterization of PU Nanospiked Gold Electrode-Based Immunosensor. DPV and EIS detection techniques were applied to characterize the construction process of the PU nanospiked gold electrode-based immunosensor. Figure 3A shows the differential pulse

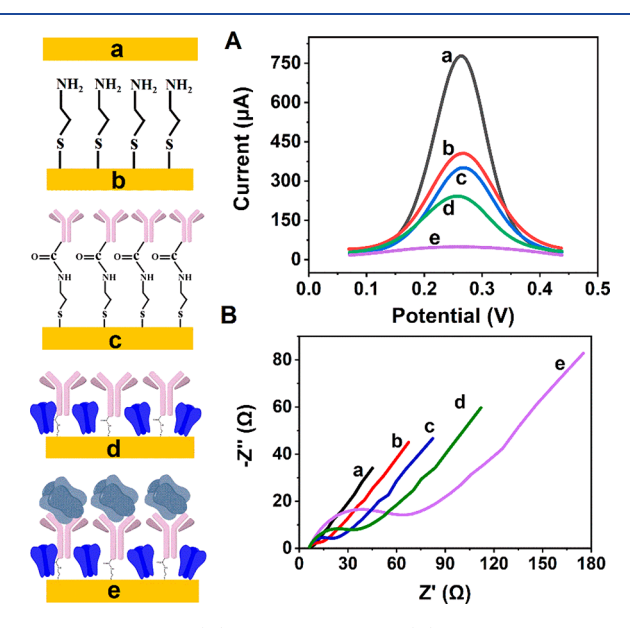


Figure 3. DPV plots (A) and Nyquist plots (B) of the immunosensor construction process. Bare PU nanospiked gold electrode (a), cystamine dihydrochloride modified PU nanospiked gold electrode (b), sdAb fixed on cystamine dihydrochloride modified PU nanospiked gold electrode (c), BSA filling nonspecific binding sites (d), and after incubating Tcd B 100 pg/mL (e).

voltammograms obtained at the bare PU nanospiked gold electrode (a), the cystamine dihydrochloride modified PU nanospiked gold electrode (b), sdAb fixed on the cystamine dihydrochloride modified PU nanospiked gold electrode (c), BSA filling nonspecific bingding sites (d), and incubating Tcd B of 100 pg/mL (e) in 5 mM K<sub>3</sub>[Fe(CN)<sub>6</sub>]/K<sub>2</sub>[Fe(CN)<sub>6</sub>] redox probe solution containing 1 M KCl under identical conditions. The PU nanospiked gold electrode had the highest peak current of 737.9  $\mu$ A. When the PU nanospiked gold electrode was modified with cystamine dihydrochloride and formed self-assembled monolayers (SAMs), the electron transfer of [Fe(CN)<sub>6</sub>]<sup>3+/2+</sup> was hindered, so the peak current decreased to 399.7  $\mu$ A. In the same way, immobilization of

sdAb and BSA also blocked the electron transfer, and the peak current decreased to 311.6 and 150.1  $\mu$ A, respectively. At this time, the PU nanospiked gold electrode-based immunosensor was completed. To confirm to the as-fabricated immunosensor being effective for detection of Tcd B, the immunosensors were incubated in Tcd B solutions of 100 pg/mL concentrations. The results are shown in Figure 3A(e); the peak current further decrease to 24.33  $\mu$ A. It revealed that Tcd B have been successfully captured by the immunosensor. The as-fabricated immunosensor was effective for detection of Tcd B.

The Nyquist plots of EIS are shown in Figure 3B. From the process of the bare PU nanospiked gold electrode (a) to after capturing the Tcd B (e), the charge transfer impedance ( $R_{\rm ct}$ ) semicircle parts of Nyquist plots) was increased. It is illustrated that every step of the construction process of the PU nanospiked gold electrode-based immunosensor was valid. The results were consistent with the DPV tests.

**Electrochemical Signal Amplification Effect of PU Nanospiked Gold Electrode.** The nanoelectrode or nanomaterial-modified electrode can greatly amplify the electrochemical detection signal. The reaction processes on the electrode surface should become faster, and this can enhance the current signal and improve the resolution for many analytes.<sup>27</sup> Here, both the PU nanospiked gold electrode and flat PU gold electrode-based immunosensor were constructed and incubated in 100 pg/mL Tcd B toxin solution. For the PU nanospiked gold electrode-based immunosensor, the peak current difference before and after incubating with Tcd B solution was 126.1 μA (Figure 4A). For the PU electrode, the peak current difference was 21.46 μA (Figure 4B). It showed that the detection signal was amplified about 6 times.

Specificity, Repeatability, Stability, and Sensitivity of the Immunosensor. Specificity is one of the most important performances of biosensors. The specificity of the PU nanospiked gold electrode-based immunosensor has been studied by testing other protein samples. All concentrations of the tested protein samples were 100 pg/mL. The incubated time was 2 h (optimization of incubated time is shown in Figure S4). As shown in Figure SA, other protein samples such as BSA, GO (glucose oxidase), Shiga toxin 2, and thrombin only have few peak current changes, but for Tcd B, the peak current change was distinct. It demonstrated that the immunosensor possesses good specificity.

The repeatability and stability of the immunosensor were also evaluated. Six PU nanospiked gold electrode-based immunosensors were fabricated; three of them were used to test Tcd B immediately, and the other three were stored in PBS at 4  $^{\circ}$ C for 2 weeks and then were used to detect the Tcd B. The results are presented in Figure 5B. The peak current of the immunosensor retained 85.12% of its initial response after storage for 2 weeks. Both fresh and stored immunosensors can effectively detect the Tcd B.

To investigate the sensitivity of the PU nanospiked gold electrode-based immunosensor, the peak current of the working electrode after incubating with different concentrations of Tcd B solutions was measured. Figure 5C shows the DPV plot of the immunosensor and after being incubated with various concentrations of Tcd B solution. The peak current change is defined as  $\Delta I = I_{(i)} - I_{(BSA)}$ , where  $I_{(BSA)}$  is peak current after the PU nanospiked gold electrode was incubated with BSA; it is the base signal of the immunosensor.  $I_{(i)}$  is the peak current of the immunosensor after being incubated in

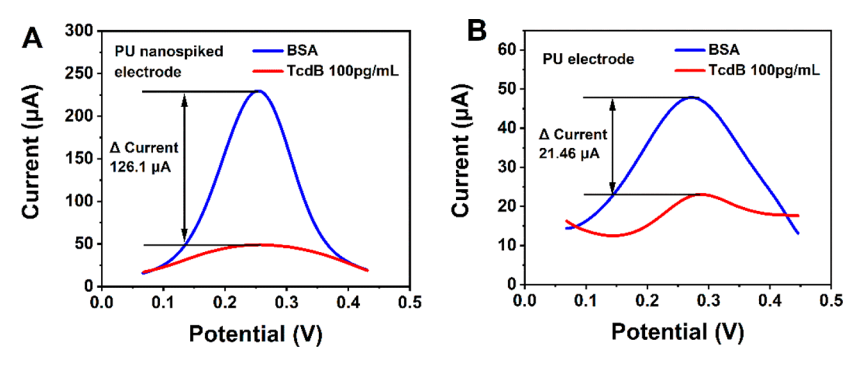


Figure 4. Peak current comparison of PU nanospiked gold electrode (A) and flat PU gold electrode (B) based immunosensor before/after incubating with 100 pg/mL Tcd B solution.

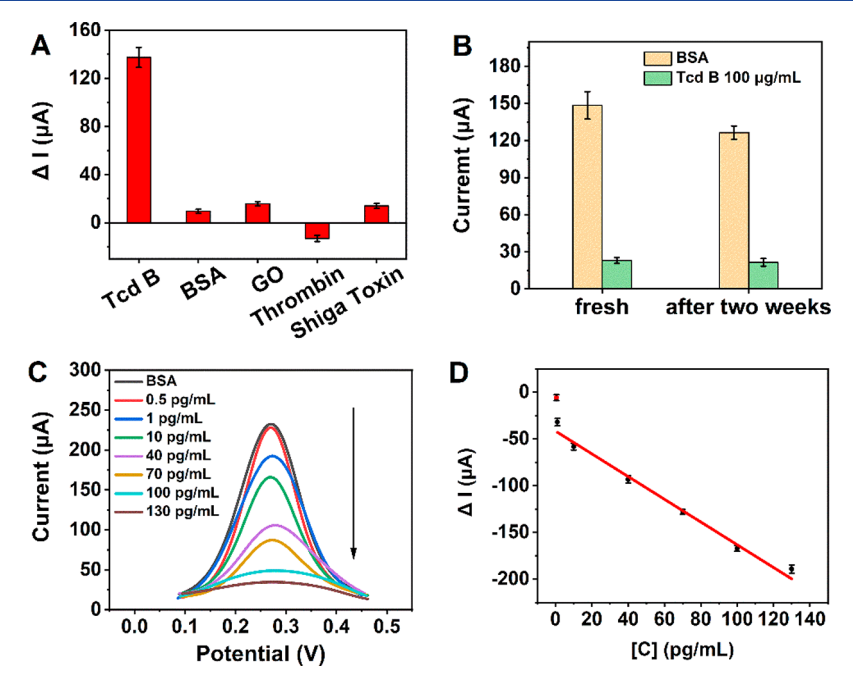


Figure 5. (A) Specificity of the imminosensor based on the PU nanospiked gold electrode. (B) Repeatability and stability of the imminosensor. (C) DPV plot of the imminosensor after incubating with different concentrations of Tcd B solution. (D) Linear regression curve of  $\Delta I$  to different concentrations of Tcd B.

Tcd B solution at different concentrations. As shown in Figure 5D, from 1 to 130 pg/mL, the  $\Delta I$  has a good linear correlation with the concentration ([C]) of Tcd B. The linear regression equation was  $\Delta I = -1.216$ [C] -41.62, with  $R^2$  of 0.9839. The LOD was measured to be 0.5 pg/mL. Compared with other electrochemical biosensor for *C. difficile* toxin, this work achieve a relatively lower LOD (Table 1).

**Real Sample Test.** To verify the performance of the developed immunosensor with the stool sample, negative stool solutions (from one stool specimen which was supplied by the

Table 1. Comparison of Different Electrochemical Measurement Techniques for *C. difficile* Toxin Detection

techniques	analyte	LOD	ref
differential pulse voltammetry	Tcd B	0.7 pg/mL	12
electrochemical impedance spectroscopy	Tcd A/B	TcdA: 0.61 pg/ mL	13
		TcdB: 0.60 pg/ mL	
differential pulse voltammetry	Tcd B	0.5 pg/mL	this work

UMASS medical school) spiked with toxin B in three different concentrations were tested. The results are presented in Table 2. It revealed that the recovery of toxin B detection for stool

Table 2. Recovery of Toxin B Detection in Stool Samples (n = 3)

added (pg/mL)	$detected \; (pg/mL)$	RSD (%)	recovery (%)
10	10.47	5.328	104.7
60	58.92	6.139	98.20
90	87.72	4.672	97.47

samples ranged from 97.47% to 104.7%. The results indicated that the biosensor has great potential to detect the Tcd B in stool samples.

#### CONCLUSIONS

In this work, a novel and simple method was proposed to prepare nanopattern in polymer-based electrode for biosensors. The repeatability of our method was better than traditional ones because of using a predefined mold. Based on this

method, PU nanospiked gold electrodes were fabricated by soft lithography. The results of SEM, CV, and DPV experiments proved their good morphology and electrochemical performance. Then, the PU nanospiked gold electrode-based label-free electrochemical immunosensor for C. difficile toxin B detection was developed. DPV was used as a detection technology for C. difficile toxin B detection, and it revealed that the immunosensor has good specificity, repeatability, and stability. Even in a label-free style, the LOD for C. difficile toxin B reached 0.5 pg/mL. In the concentration range 1-130 pg/mL, a linear relationship was observed between the peak current and concentration of TcdB. The linear regression equation was  $\Delta I = -1.216$ [C] - 41.62 (the correlation coefficient  $R^2$  was 0.9839). The signal was amplified about 6 times compared with flat PU gold electrode-based immunosensor. Owing to the low cost and simple processing, the PU nanospiked gold electrode-based immunosensor can be used a disposable electrochemical sensor for toxin B rapid detection.

#### ASSOCIATED CONTENT

#### **S** Supporting Information

The Supporting Information is available free of charge at https://pubs.acs.org/doi/10.1021/acsanm.9b02001.

(1) Characterization of PU nanospiked gold electrode by energy dispersive X-ray spectroscopy (EDS); (2) cyclic voltammograms in 0.5 M H<sub>2</sub>SO<sub>4</sub> and calculation of electrochemical active area; (3) stability of the electrode with cyclic voltammetry; (4) optimization of experimental conditions (PDF)

#### AUTHOR INFORMATION

#### **Corresponding Author**

\*E-mail: szhou@wpi.edu (H.S.Z.).

ORCID

Feiyun Cui: 0000-0001-5055-1423

Notes

The authors declare no competing financial interest.

## ■ ACKNOWLEDGMENTS

This work was supported by the National Science Foundation (CBET-1805514) to H.S.Z.

## REFERENCES

- (1) Pollock, N. R. Ultrasensitive Detection and Quantification of Toxins for Optimized Diagnosis of Clostridium Difficile Infection. *J. Clin. Microbiol.* **2016**, *54* (2), 259–264.
- (2) Magill, S. S.; Edwards, J. R.; Bamberg, W.; Beldavs, Z. G.; Dumyati, G.; Kainer, M. A.; Lynfield, R.; Maloney, M.; McAllister-Hollod, L.; Nadle, J.; Ray, S. M.; Thompson, D. L.; Wilson, L. E.; Fridkin, S. K. Multistate Point-Prevalence Survey of Health Care—Associated Infections. N. Engl. J. Med. 2014, 370 (13), 1198–1208.
- (3) Saade, E.; Deshpande, A.; Kundrapu, S.; Sunkesula, V. C. K.; Guerrero, D. M.; Jury, L. A.; Donskey, C. J. Appropriateness of Empiric Therapy in Patients with Suspected Clostridium Difficile Infection. *Curr. Med. Res. Opin.* **2013**, 29 (8), 985–988.
- (4) Barbut, F.; Surgers, L.; Eckert, C.; Visseaux, B.; Cuingnet, M.; Mesquita, C.; Pradier, N.; Thiriez, A.; Ait-Ammar, N.; Aifaoui, A.; Grandsire, E.; Lalande, V. Does a Rapid Diagnosis of Clostridium Difficile Infection Impact on Quality of Patient Management? *Clin. Microbiol. Infect.* **2014**, 20 (2), 136–144.
- (5) Kuehne, S. A.; Cartman, S. T.; Heap, J. T.; Kelly, M. L.; Cockayne, A.; Minton, N. P. The Role of Toxin A and Toxin B in Clostridium Difficile Infection. *Nature* **2010**, *467*, 711.

- (6) Lyras, D.; O'Connor, J. R.; Howarth, P. M.; Sambol, S. P.; Carter, G. P.; Phumoonna, T.; Poon, R.; Adams, V.; Vedantam, G.; Johnson, S.; Gerding, D. N.; Rood, J. I. Toxin B is Essential for Virulence of Clostridium Difficile. *Nature* **2009**, *458*, 1176–1179.
- (7) Gateau, C.; Couturier, J.; Coia, J.; Barbut, F. How to: Diagnose Infection Caused by Clostridium Difficile. *Clin. Microbiol. Infect.* **2018**, 24 (5), 463–468.
- (8) Crobach, M. J. T.; Planche, T.; Eckert, C.; Barbut, F.; Terveer, E. M.; Dekkers, O. M.; Wilcox, M. H.; Kuijper, E. J. European Society of Clinical Microbiology and Infectious Diseases: Update of the Diagnostic Guidance Document for Clostridium Difficile Infection. *Clin. Microbiol. Infect.* **2016**, *22*, S63–S81.
- (9) Song, L.; Zhao, M.; Duffy, D. C.; Hansen, J.; Shields, K.; Wungjiranirun, M.; Chen, X.; Xu, H.; Leffler, D. A.; Sambol, S. P.; Gerding, D. N.; Kelly, C. P.; Pollock, N. R. Development and Validation of Digital Enzyme-Linked Immunosorbent Assays for Ultrasensitive Detection and Quantification of Clostridium difficile Toxins in Stool. *J. Clin. Microbiol.* **2015**, 53 (10), 3204–3212.
- (10) Sandlund, J.; Bartolome, A.; Almazan, A.; Tam, S.; Biscocho, S.; Abusali, S.; Bishop, J. J.; Nolan, N.; Estis, J.; Todd, J.; Young, S.; Senchyna, F.; Banaei, N. Ultrasensitive Detection of Clostridioides difficile Toxins A and B by Use of Automated Single-Molecule Counting Technology. J. Clin. Microbiol. 2018, 56 (11), e00908.
- (11) Syahir, A.; Usui, K.; Tomizaki, K.-Y.; Kajikawa, K.; Mihara, H. Label and Label-Free Detection Techniques for Protein Microarrays. *Microarrays* **2015**, 4 (2), 228–244.
- (12) Fang, Y. S.; Chen, S. Y.; Huang, X. J.; Wang, L. S.; Wang, H. Y.; Wang, J. F. Simple Approach for Ultrasensitive Electrochemical Immunoassay of Clostridium Difficile Toxin B Detection. *Biosens. Bioelectron.* **2014**, 53, 238–244.
- (13) Zhu, Z.; Shi, L.; Feng, H.; Susan Zhou, H. Single Domain Antibody Coated Gold Nanoparticles as Enhancer for Clostridium Difficile Toxin Detection by Electrochemical Impedance Immunosensors. *Bioelectrochemistry* **2015**, *101*, 153–158.
- (14) Han, S.; Liu, W.; Yang, S.; Wang, R. Facile and Label-Free Electrochemical Biosensors for MicroRNA Detection Based on DNA Origami Nanostructures. ACS Omega 2019, 4 (6), 11025–11031.
- (15) Moghaddam, H. M.; Beitollahi, H.; Dehghannoudeh, G.; Forootanfar, H. A Label-Free Electrochemical Biosensor Based on Carbon Paste Electrode Modified with Graphene and ds-DNA for the Determination of the Anti-Cancer Drug Tamoxifen. *J. Electrochem. Soc.* 2017, 164 (7), B372–B376.
- (16) Subak, H.; Ozkan-Ariksoysal, D. Label-Free Electrochemical Biosensor for the Detection of Influenza Genes and the Solution of Guanine-Based Displaying Problem of DNA Hybridization. *Sens. Actuators, B* **2018**, 263, 196–207.
- (17) Thangamuthu, M.; Santschi, C.; Martin, O. J. F. Label-Free Electrochemical Immunoassay for C-Reactive Protein. *Biosensors* **2018**, 8 (2), 34.
- (18) Kempahanumakkagari, S.; Vellingiri, K.; Deep, A.; Kwon, E. E.; Bolan, N.; Kim, K.-H. Metal—Organic Framework Composites as Electrocatalysts for Electrochemical Sensing Applications. *Coord. Chem. Rev.* **2018**, 357, 105—129.
- (19) Baig, N.; Sajid, M.; Saleh, T. A. Recent Rrends in Nanomaterial-Modified Electrodes for Electroanalytical Applications. *TrAC, Trends Anal. Chem.* **2019**, *111*, 47–61.
- (20) Yang, G.; Zhou, B.; Wang, J.; He, X.; Sun, X.; Nie, W.; Tzipori, S.; Feng, H. Expression of Recombinant Clostridium Difficile Toxin A and B in Bacillus Megaterium. *BMC Microbiol.* **2008**, *8*, 192.
- (21) Yang, Z.; Schmidt, D.; Liu, W.; Li, S.; Shi, L.; Sheng, J.; Chen, K.; Yu, H.; Tremblay, J. M.; Chen, X.; Piepenbrink, K. H.; Sundberg, E. J.; Kelly, C. P.; Bai, G.; Shoemaker, C. B.; Feng, H. A Novel Multivalent, Single-Domain Antibody Targeting TcdA and TcdB Prevents Fulminant Clostridium Difficile Infection in Mice. *J. Infect. Dis.* **2014**, *210* (6), 964–72.
- (22) Xu, Q.; Mayers, B. T.; Lahav, M.; Vezenov, D. V.; Whitesides, G. M. Approaching Zero: Using Fractured Crystals in Metrology for Replica Molding. J. Am. Chem. Soc. 2005, 127 (3), 854–855.

- (23) Huo, H.; Shen, M.; Ebstein, S. M.; Guthermann, H. Surface-Assisted Laser Desorption and Ionization Mass Spectrometry Using Low-Cost Matrix-Free Substrates. *J. Mass Spectrom.* **2011**, 46 (9), 859–64.
- (24) Shen, M. Y.; Crouch, C. H.; Carey, J. E.; Mazur, E. Femtosecond Laser-Induced Formation of Submicrometer Spikes on Silicon in Water. *Appl. Phys. Lett.* **2004**, *85* (23), 5694–5696.
- (25) Qin, D.; Xia, Y.; Whitesides, G. M. Soft Lithography for Microand Nanoscale Patterning. *Nat. Protoc.* **2010**, *5* (3), 491–502.
- (26) Elshafey, R.; Tavares, A. C.; Siaj, M.; Zourob, M. Electrochemical Impedance Immunosensor Based on Gold Nanoparticles—Protein G for the Detection of Cancer Marker Epidermal Growth Factor Receptor in Human Plasma and Brain Tissue. *Biosens. Bioelectron.* **2013**, *50*, 143–149.
- (27) Donten, M.; Stojek, Z. Nanoparticles and Nanostructured Materials Used in Modification of Electrode Surfaces. In Functional Nanoparticles for Bioanalysis, Nanomedicine, and Bioelectronic Devices Vol. 1; American Chemical Society: 2012; Vol. 1112, pp 313–325.